Proton Decay of ^{21}Na for ^{20}Ne Energy Levels

M. J. Kim, K. Y. Chae,* and S. M. Cha

Department of Physics, Sungkyunkwan University, Suwon 16419, Korea

S. H. Ahn

Department of Physics and Astronomy,

University of Tennessee, Knoxville, Tennessee 37996, USA

D. W. Bardayan

Department of Physics, University of Notre Dame, Notre Dame, Indiana 46556, USA

K. A. Chipps

Colorado School of Mines, Golden, Colorado 80401, USA and

Physics Division, Oak Ridge National Laboratory,

Oak Ridge, Tennessee 37831, USA

J. A. Cizewski, M. E. Howard, B. Manning, and A. Ratkiewicz

Department of Physics and Astronomy, Rutgers University,

New Brunswick, New Jersey 08903, USA

R. L. Kozub

Department of Physics, Tennessee Technological

University, Cookeville, Tennessee 38505, USA

K. Kwak

Department of Physics, School of Natural Science,

Ulsan National Institute of Science and Technology (UNIST), Ulsan 44919, Korea

M. Matos

Department of Physics and Astronomy,

Louisiana State University, Baton Rouge, LA 70803, USA

P. D. O'Malley and S. Strauss

Department of Physics and Astronomy, Rutgers University,

New Brunswick, New Jersey 08903, USA and

Department of Physics, University of Notre Dame, Notre Dame, Indiana 46556, USA

S. D. Pain, S. T. Pittman, and M. S. Smith

Physics Division, Oak Ridge National Laboratory,

Oak Ridge, Tennessee 37831, USA

W. A. Peters

Oak Ridge Associated Universities, Oak Ridge, Tennessee 37831, USA

Abstract

The ^{24}Mg(p,α)^{21}Na transfer reaction has been previously studied for a spectroscopic study of ^{21}Na [Cha *et al.*, Phys. Rev. C **96**, 025810 (2017)]. In this follow-up analysis, the proton decays of the excited states of the radionuclide ^{21}Na, which were measured simultaneously, are reported. By investigating the coincidence between the reaction α-particles and decay protons, we were able to identify three groups of events that are associated with the energy levels in ^{20}Ne. The ^{20}Ne excitation energy plot was obtained as a result. The four lowest known energy levels in ^{20}Ne (the ground state and excited states at E_x = 1.633, 4.247 and 4.966 MeV) were clearly observed.

PACS numbers: 27.30.+t, 25.40.Hs, 23.50.+z, 29.30.Ep

Keywords: Transfer reaction, Proton decay, Excitation energy, Radionuclide

*Electronic address: kchae@skku.edu; Fax: +82-31-290-7055

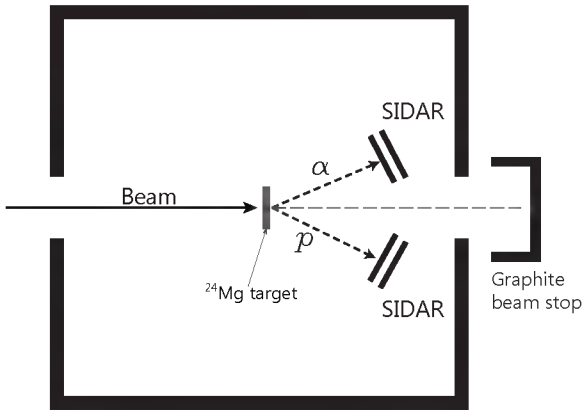

FIG. 1: Schematic diagram of the experimental setup.

I. INTRODUCTION

The study of a transfer reaction is a powerful experimental tool in nuclear spectroscopy. The measurement of the energy and angular distributions of the reaction products reveal very important properties, such as the excitation energy, spin and parity, and spectroscopic information. Many types of transfer reactions, including (p,d), (p,t), $(p,^3\mathrm{He})$, (p,α), (d,p), (d,t), and so forth, have been utilized both in normal and inverse kinematics for spectroscopic studies [1]. When radionuclides are produced as the result of transfer reactions, measuring the properties of their decays is useful, as shown in Refs. [2–7]. The $^{24}\mathrm{Mg}(p,\alpha)^{21}\mathrm{Na}$ transfer reaction has been previously studied at the Holifield Radioactive Ion Beam Facility (HRIBF) [8] of the Oak Ridge National Laboratory (ORNL) for the spectroscopic study of the radionuclide ^{21}Na [9], as summarized in the following paragraphs. In this paper, the proton decay of ^{21}Na, which was a by-product of the $^{24}\mathrm{Mg}(p,\alpha)^{21}\mathrm{Na}$ reaction measurement, is reported.

A schematic diagram of the $^{24}\mathrm{Mg}(p,\alpha)^{21}\mathrm{Na}$ experimental setup is shown in Figure 1. A 31-MeV proton beam from the tandem accelerator bombarded isotopically enriched (99.9%) ^{24}Mg solid targets. Recoiling charged particles were detected at forward angles by using a silicon strip detector array (SIDAR) [10], which was composed of four trapezoidal wedges of $\Delta E{-}E$ telescopes. Each telescope was configured with a thin (100 μm-thick) detector backed by a thick (1000 μm-thick) detector. Since each detector is segmented into 16 annular strips, the angular distribution could be extracted simultaneously. The angular range covered by the SIDAR was $17^\circ < \theta_{\mathrm{lab}} < 44^\circ$. Detected light charged particles could be identified by using a standard energy loss technique, as shown in Figure 2 which was obtained at $\theta_{\mathrm{lab}} =$

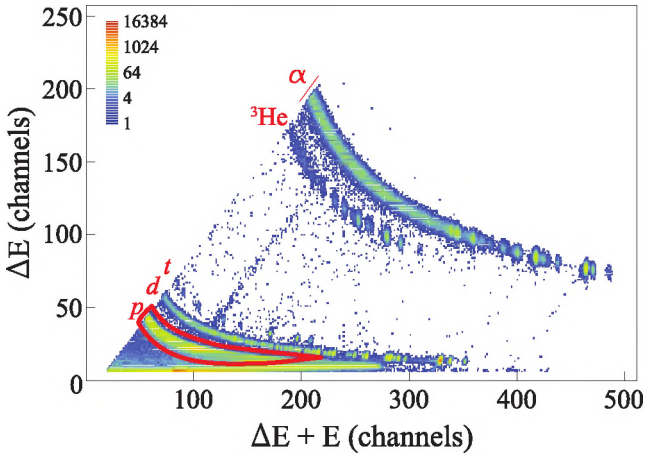

FIG. 2: (Color online) Particle identification plot obtained at $\theta_{lab} = 27.2°$ is shown. Particles falling in the red gate were identified as protons. The light charged particles from the reaction (p, d, t, ^{3}He, and α) are clearly identified.

27.2°.

A total of 12 energy levels in ^{21}Na were identified in the energy range of $E_x \lessapprox 7.2$ MeV. Two levels, one located at $E_x = 6.594$- and the other at 7.132-MeV, were observed for the first time. By comparing the observed angular distributions with theoretical distorted wave Born approximation (DWBA) calculations, the spins and parities of the identified levels were constrained. The newly constrained spin values were then used to calculate the astrophysical ^{17}F(α,p)^{20}Ne reaction rate at stellar temperature. Calculations indicated that the reaction rate was increased by a factor of five at $T = 0.25$ GK owing to the newly found 7.132-MeV level.

II. COINCIDENCE BETWEEN DECAY PROTONS AND REACTION α-PARTICLES

As described in the previous section, the experimental setup was optimized for studying the ^{24}Mg(p,α)^{21}Na reaction: a proton beam energy of 31 MeV, a ^{24}Mg target thickness of about 520 μg/cm^2, the thickness of each layer of the silicon detector (100 μm for ΔE and 1000 μm for E), and the angles subtended by the silicon detector array ($17° < \theta_{\rm lab} < 44°$). As a result, energetic protons with energies above ~ 7.2 MeV punched through the E layer, which resulted in a "back-bending" locus, as shown in Figure 2. In the present analysis,

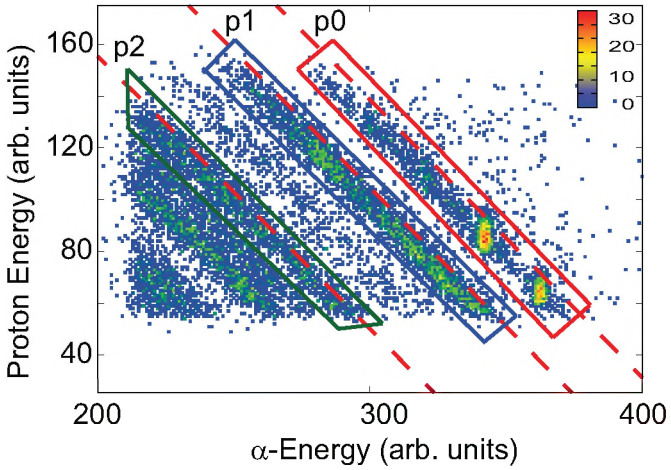

FIG. 3: (Color online) Decay proton energy versus coincident reaction α-particle energy spectrum. Several diagonal groups of events, which are associated with the ground (p0), first (p1), and second (p2) excited states in ^{20}Ne, are evident in the figure.

therefore, only low energy protons falling in the gate of the figure were used. As previously done by Chipps *et al.* in the ^{14}N$(p,t)^{12}$N$^*(p)^{11}$C* study [6], we simultaneously detected emitted protons from the decay of ^{21}Na and α-particles from the ^{24}Mg$(p,\alpha)^{21}$Na reaction.

The energy response of each silicon strip was calibrated using an α-emitting radioactive source composed of ^{239}Pu (5.157 MeV), ^{241}Am (5.486 MeV), and ^{244}Cm (5.805 MeV). Since the energies of the α-particles observed in the present work ranged from $\sim$ 9.8 MeV to $\sim$ 23.3 MeV, well above the α source calibration range, the α-energy spectra obtained at each SIDAR strip were internally calibrated by using four well-known energy levels of ^{21}Na located at E_x = 0.332, 2.798, 4.419, and 6.879 MeV. As described in Ref. [9], the internal energy calibrations resulted in very good agreement of the extracted excitation energies with those from the literature. For the energies of protons, such additional energy calibrations could not be performed since the proton energy spectra from the reaction measurements were rather featureless. Because the energy range of observed protons is from about 2.4 to 7.2 MeV, the energy gains obtained from the calibrations with α-emitting source worked well.

Some ^{21}Na levels that are populated through the ^{24}Mg$(p,\alpha)^{21}$Na transfer reaction decay to one of the levels in ^{20}Ne by emitting protons. Figure 3 was obtained by requiring coincidence between the decay protons and reaction α particles and shows all coincident events. Several diagonal groups of events, which are evident in the figure, are associated with the ground (J^π

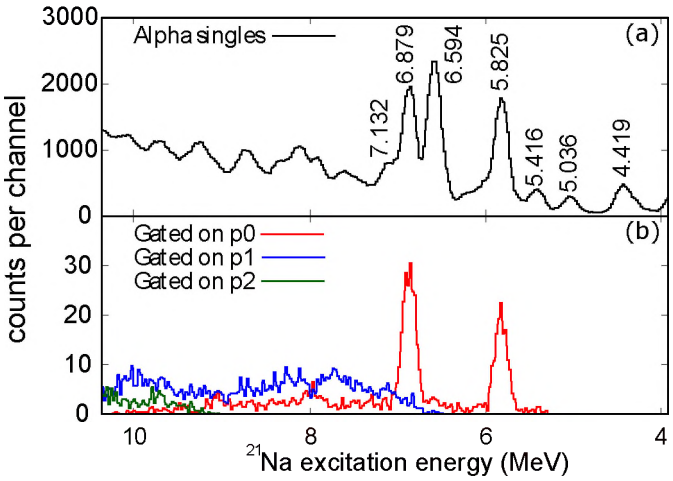

FIG. 4: (Color online) (a) ^{21}Na excitation energy spectrum obtained from the ^{24}Mg(p,α)^{21}Na reaction measurement. (b) Spectra gated on decay proton coincidences : red for p0, blue for p1 and green for p2. Each identified energy level is labeled with its excitation energy in MeV, which is adopted from Ref. [9].

$= 0^+$, red gate), first ($E_x = 1.633$ MeV, $J^\pi = 2^+$, blue gate), and second ($E_x = 4.247$ MeV, $J^\pi = 4^+$, green gate) excited states in ^{20}Ne. Each group is labeled as p0, p1, or p2. Dashed lines show the regions where the events associated with each ^{20}Ne level are expected from kinematics. Especially for the p0 group, which originate from different ^{21}Na states, several groups are clearly shown. For instance, the lower right group in the p0 gate represents events from the proton decay of the $E_x = 5.825$ MeV level of ^{21}Na. Another group appearing at about channel 80 on the y-axis shown events from the $E_x = 6.879$ MeV level.

III. ^{20}Ne STATES

The ^{21}Na excitation energy spectrum obtained from the ^{24}Mg(p,α)^{21}Na reaction measurement is shown in Figure 4 (a). Each identified energy level is labeled with its excitation energy in MeV; the values are adopted from Ref. [9]. The α-energy spectra were extracted from all 16 strips (angles) and internally calibrated first at each angle and then converted to a ^{21}Na excitation energy plot by using the known detector geometry and reaction kinematics. The figure shows the energy spectrum summed over all angles.

The summed spectra gated on decay proton coincidences are shown in Figure 4(b): red for p0, blue for p1, and green for p2. By comparing the number of counts in Figure 4(a) to

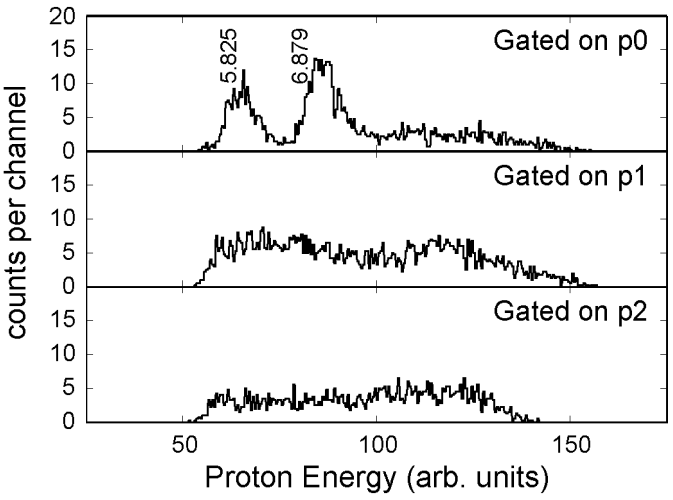

FIG. 5: Proton energy spectra of coincident events for each gate of Figure 3. The graphs are associated with the ground state (p0, top), first (1.633 MeV, p1, middle) excited state, and second (4.247 MeV, p2, bottom) excited state of ^{20}Ne. Apparent peaks in the top spectrum are labelled with the corresponding ^{21}Na excitation energies.

that in Figure 4(b), we found that only about 2% of the α particles from the ^{24}Mg(p,α)^{21}Na transfer reaction had coincident protons. If the precise proton branching ratios are to be deduced, however, the geometric detection efficiency should be considered. Due to the proton threshold energy in ^{21}Na (2.432 MeV) and the discriminator threshold, any ^{21}Na energy level located above $E_x \sim 5.2$ MeV could be observed in the present proton-alpha coincidence plot. As shown in Figure 4(b), however, only two energy levels, one at $E_x = 5.825$ MeV and the other at $E_x = 6.879$ MeV, were clearly identified in the p0-gated α spectrum. No obvious structure was observed for the p1 and the p2 groups.

Figure 5 shows the proton energy spectra of coincident events for each gate of Figure 3. Events falling in each gate were projected onto the y-axis to obtain the spectra. Each graph is associated with the ground state (p0, top) and the first (1.633 MeV, p1, middle) and the second (4.247 MeV, p2, bottom) excited state of ^{20}Ne. Apparent peaks in the top spectrum are labelled with the corresponding ^{21}Na excitation energies. For the cases of the spectra associated with the p1 and p2 groups, however, no clear structure was observed. The energy resolution of the spectrum is a bit worse than that of α-energy spectrum due to the lack of internal energy calibration information, as we were described above. However, since the energy range of the decay proton of interest is close to that of the α particles used

TABLE I: The measured and the calculated values of the decay proton energy (E_p) are summarized for two identified energy levels of ^{21}Na. The uncertainty in E_p includes the energy resolution of the silicon detectors and the quality of the fit. All energies are in MeV.

Transition	E_p measured	E_p expected
$5.825 \rightarrow 0.000$	3.137 ± 0.42	3.394
$6.879 \rightarrow 0.000$	4.162 ± 0.53	4.448

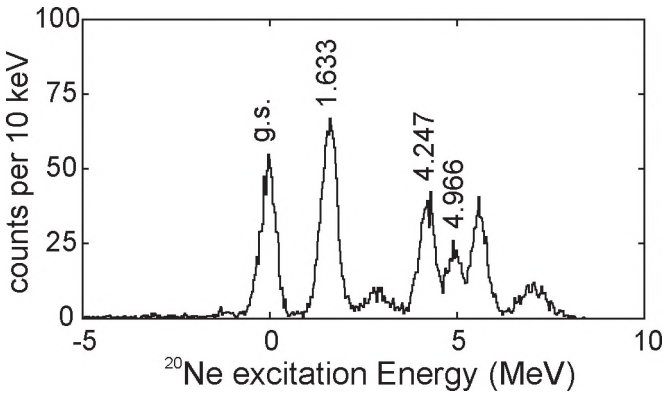

FIG. 6: The excitation energy in ^{20}Ne was reconstructed by using the kinetic energies of the reaction α-particles and the decay protons.

for detector calibration, the reconstructed proton energies would be reasonably reproduced by using this procedure.

Each peak identified in the top panel of Figure 5 was fitted by assuming a Gaussian distribution. The measured value of the decay proton energy (E_p) was taken from the centroid of the distribution. The measured E_p was then compared with the expected value that had been calculated by adopting the proton threshold energy in ^{21}Na of 2.432 MeV [11] and the ^{20}Ne level energies from Ref. [12]. The uncertainty in E_p includes both the energy resolution of the silicon detectors and the quality of the fit. Since the p1 and the p2 channels do not show any structure due to low statistics and rather worse energy resolution in proton spectrum, only the two peaks identified from the p0 channel were considered. The results are summarized in Table I. All energies are in MeV.

The excitation energy in ^{20}Ne was reconstructed by using the kinetic energies of the reaction α-particle and the decay proton, as shown in Figure 6. Four known energy levels are clearly identified: the ground state and the excited states located at $E_x = 1.633$-, 4.247-, and

TABLE II: Excitation energies and uncertainties of energy levels identified in the present work. The level energy values from Ref. [12] are also shown for reference. All energies are in MeV.

E_x (present work)	E_x (Ref. [12])
0.000 ± 0.49^a	0
1.633 ± 0.46^a	1.633
2.92 ± 0.91	-
4.247 ± 0.51^a	4.247
4.966 ± 0.41^a	4.966
5.64 ± 0.50	5.621 + 5.787
7.04 ± 0.80	-

[a]This energy level is used for the internal energy calibration.

4.966-MeV, respectively. These levels were used for internal energy calibration. The peaks are labeled with known excitation energies, which are adopted from Ref. [12]. Extracted excitation energies and uncertainties of identified the levels are summarized in Table II. Peaks were observed between E_x = 1.633 MeV and 4.247 MeV. The excitation energy of 2.92 ± 0.91 MeV was deduced by assuming the peak is caused by an energy level in ^{20}Ne, which has not been reported so far. However, other possibilities that might produce protons in this energy range should be thoroughly considered. As had been successfully done in previous particle decay studies [2–7], the proton branching ratios will be extracted as well by considering geometric detection efficiencies for the four identified energy levels in the excitation energy plot.

IV. CONCLUSION AND FUTURE PLAN

Decay protons from excited states in ^{21}Na, which originated from the ^{24}Mg(p,α)^{21}Na transfer reaction, were analyzed. By requiring coincidence between the reaction α-particles and the decay protons, we are able to identify three groups of events, which are associated with the ground (p0), first (p1, E_x = 1.633 MrV), and second (p2, E_x = 4.247 MeV) excited states in ^{20}Ne. The excitation energy in ^{20}Ne was then reconstructed by using the kinetic energies of the particles. The populations of the four lowest energy levels in ^{20}Ne

were evident from the spectrum. The peak-like structure appearing between the first and the second excited states has never been reported before. Calculations indicate that a excitation energy of $E_x = 2.92 \pm 0.91$ MeV would be deduced from the present work if the peak were assumed to have originated from an energy level of ^{20}Ne.

To ensure that the peaks arise from an excited state of ^{20}Ne, we will perform more precise internal energy calibrations and careful consideration of the background. Contaminating elements such as ^{12}C, ^{14}N, and ^{16}O are often found in solid targets. Therefore, for instance, the ^{14}N$(p,\alpha)^{11}$C$^*(p)^{10}$B* channel will be investigated. The proton branching ratios of the identified levels in ^{21}Na will also be deduced by considering the geometric detection efficiency and more.

Acknowledgments

This work was supported by a National Research Foundation of Korea (NRF) grant funded by the Korea government Ministry of Education, Science, and Technology (MEST) (Nos. NRF-2013M7A1A1075764, NRF-2020R1A2C1005981, and NRF-2019R1F1A1058370). This research was supported in part by the National Nuclear Security Administration under the Stewardship Science Academic Alliances program through the U.S. DOE Cooperative Agreement No. DE-FG52-08NA28552 with Rutgers University and Oak Ridge Associated Universities. This work was also supported in part by the Office of Nuclear Physics, Office of Science of the U.S. DOE under Contracts No. DE-FG02-96ER40955 with Tennessee Technological University, No. DE-FG02-96ER40983 with the University of Tennessee, and DE-AC-05-00OR22725 at Oak Ridge National Laboratory, and by the National Science Foundation under Contract No. PHY-1713857 with University of Notre Dame and NO. PHY-1404218 with Rutgers University.

---

[1] D. W. Bardayan, J. Phys. G: Nucl. Phys. **43**, 043001 (2016).

[2] W. P. Tan, J. L. Fisker, J. Gorres, M. Couder, and M. Wiescher, Phys. Rev. Lett. **98**, 242503 (2007).

[3] C. M. Deibel, J. A. Clark, R. Lewis, A. Parikh, P. D. Parker, and C. Wrede, Phys. Rev. C **80**, 035806 (2009).

[4] K. A. Chipps *et al.*, Phys. Rev. C **82**, 045803 (2010).

[5] K. A. Chipps *et al.*, Phys. Rev. C **86**, 014329 (2012).

[6] K. A. Chipps *et al.*, Phys. Rev. C **95**, 044319 (2017).

[7] D. W. Bardayan *et al.*, J. Phys. Conf. Ser. **1308**, 012004 (2019).

[8] J. R. Beene *et al.*, J. Phys. G: Nucl. Part. Phys. **38**, 024002 (2011).

[9] S. M. Cha *et al.*, Phys. Rev. C **96**, 025810 (2017).

[10] D. W. Bardayan *et al.*, Phys. Rev. C **63**, 065802 (2001).

[11] R. B. Firestone, Nucl. Data Sheets **127**, 1 (2015).

[12] D. R. Tilley, C. M. Cheves, J. H. Kelley, S. Raman, and H. R. Weller, Nucl. Phys. A **636**, 249 (1998).